

Glycine 699 is Pivotal for the Motor Activity of Skeletal Muscle Myosin

Fumi Kinose, Sharon X. Wang, Usha S. Kidambi, Carole L. Moncman and Donald A. Winkelmann

Department of Pathology, Robert Wood Johnson Medical School, Piscataway, New Jersey 08854

Abstract. Myosin couples ATP hydrolysis to the translocation of actin filaments to power many forms of cellular motility. A striking feature of the structure of the muscle myosin head domain is a 9-nm long "lever arm" that has been postulated to produce a 5–10-nm power stroke. This motion must be coupled to conformational changes around the actin and nucleotide binding sites. The linkage of these sites to the lever arm has been analyzed by site-directed mutagenesis of a conserved glycine residue (G699) found in a bend joining two helices containing the highly reactive and mobile cysteine residues, SH1 and SH2. Alanine mutagenesis of this glycine (G699A) dramatically alters the motor activity of skeletal muscle myosin, inhibiting the velocity of actin filament movement by >100-fold. Analysis of the defect in the G699A mutant myosin is consistent with a marked slowing of the transition within the motor domain from a strong binding to a weak binding interaction with actin. This result is interpreted in terms of the role of this residue (G699) as a pivot point for motion of the lever arm. The recombinant myosin used in these experiments has been produced in a unique expression

system. A shuttle vector containing a regulated muscle-specific promoter has been developed for the stable expression of recombinant myosin in C2C12 cells. The vector uses the promoter/enhancer region, the first two and the last five exons of an embryonic rat myosin gene, to regulate the expression of an embryonic chicken muscle myosin cDNA. Stable cell lines transfected with this vector express the unique genetically engineered myosin after differentiation into myotubes. The myosin assembles into myofibrils, copurifies with the endogenous myosin, and contains a complement of muscle-specific myosin light chains. The functional activity of the recombinant myosin is readily analyzed with an *in vitro* motility assay using a species-specific anti-S2 mAb to selectively assay the recombinant protein. This expression system has facilitated manipulation and analysis of the skeletal muscle myosin motor domain and is also amenable to a wide range of structure–function experiments addressing questions unique to the muscle-specific cytoarchitecture and myosin isoforms.

MYOSIN is the crucial motor component of muscle contraction and essential to numerous forms of cellular movements (Warrick and Spudich, 1987; Cheney et al., 1993). The muscle-specific isoform of this motor molecule assembles into bipolar thick filaments that interdigitate with thin actin filaments in a highly ordered cytoskeletal structure called the myofibril (Lowey, 1994). There is now a large family of actin-based motors that have been identified based on sequence and functional homology with the motor domain of skeletal muscle myosin (Hammer, 1991). They share a common minimal motor domain with >50% sequence homology with muscle myosin. Those myosins that have been isolated and assayed have an actin-activated ATPase that couples ATP hydrolysis to the translocation of actin filaments.

The structure of the head domain of chicken skeletal

muscle myosin reveals an asymmetric molecule with secondary structure dominated by many long α -helices (Rayment et al., 1993b). One exceptionally long helix spans 85 Å and is stabilized by interactions with the myosin light chains. Based on several lines of evidence, it has been proposed that this light chain binding domain acts as a semi-rigid "lever arm" to amplify and transmit conformational changes in the nucleotide and actin binding sites of the myosin head (Lowey et al., 1993b; Rayment et al., 1993a; Jontes et al., 1995; Whittaker et al., 1995). The nucleotide and actin binding sites are formed by ~780 residues from the amino terminus of the myosin heavy chain. This fragment represents the minimal motor domain and can support limited sliding movement of actin filaments (Itakura et al., 1993; Waller et al., 1995).

A significant feature of the myosin structure is a deep cleft ~4 nm long that splits the actin binding site between two subdomains and terminates beneath the nucleotide binding pocket (Rayment et al., 1993a, b). Closure of the cleft on binding to actin and its modulation by nucleotide have been proposed as a mechanism for coupling actin ac-

Address all correspondence to Donald A. Winkelmann, Department of Pathology, University of Medicine & Dentistry of New Jersey–Robert Wood Johnson Medical School, 675 Hoes Lane, Piscataway, NJ 08854. Tel.: (908) 235-4759. Fax: (908) 235-4825. e-mail: daw@pleiad.umdj.edu.

tivation of the myosin ATPase activity to movement and force production (Rayment et al., 1993a; Spudich, 1995). It has been postulated that these changes are linked to the movement of the long lever arm to produce a 5–10-nm power stroke (Rayment et al., 1993a; Finer et al., 1994; Spudich, 1995).

Support for this hypothesis comes from experiments designed to alter the mechanical properties of the lever arm. Weakening the lever arm by removal of one or both light chains results in a reduction in actin filament velocity and force production (Lowey et al., 1993b; VanBuren et al., 1994). Truncation of the lever arm by removal of one light chain binding site also produces a reduction in filament velocity (Uyeda and Spudich, 1993), and addition of an extra binding site, lengthening the lever arm, increases the velocity (Uyeda et al., 1996). The truncated motor domains completely lacking the light chain binding helix show a large decrease in filament velocity with little effect on ATPase activity (Itakura et al., 1993; Waller et al., 1995). Structural evidence for the lever arm hypothesis has come from helical reconstruction of actin filaments decorated with myosin heads (Jontes et al., 1995; Whittaker et al., 1995). When ADP is bound to the acto–myosin complex, the light chain binding domain moves like a rigid lever by 32°. Modeling the movement places the “pivot point” of the lever in the vicinity of several important structural elements in the motor domain, including two helices containing the reactive sulfhydryls.

The goal of this work is to localize the pivot point where the lever arm emerges from the motor domain. Our attention was directed to the two short helices carrying the reactive sulfhydryls, SH1 and SH2 (C707 and C697), because they are located in a highly conserved segment of the motor domain, which appears to be highly mobile as well. These two sulfhydryls can be cross-linked by a variety of reagents bridging distances of 4–18 Å (Wells et al., 1980). Cross-linking SH1 and SH2 can trap nucleotide in the active site (Wells and Yount, 1979). Chemical modification of SH1 or SH2 dramatically alters myosin ATPase activity and actin binding affinity, and nucleotide binding alters the separation between SH1 and SH2 (Reisler et al., 1974; Pemrick and Weber, 1976; Dalbey et al., 1983). These results suggested that SH1 and SH2 would reside on a flexible loop. However, these residues are located on well-defined α -helix segments. The helices in the myosin structure are joined by a turn, and the sulfhydryls are separated by 18 Å (Rayment et al., 1993b). A conserved glycine residue (G699) that is found in all myosin sequences is located in the turn that links the two reactive sulfhydryl helices, and we reasoned that this residue might be key to the mobility of these sulfhydryls. Furthermore, the SH1-containing helix is linked to the lever arm, so motion within this region could be directly coupled to force transmission.

We have tested this idea by using alanine mutagenesis to perturb the motion around this highly conserved glycine (G699). To accomplish this, we have developed a unique approach for the preparation of fast skeletal muscle myosin that is based on regulated expression of a recombinant myosin gene in a mouse myogenic cell line that differentiates and forms contractile myotubes. This expression system was combined with a simple technique for selective isolation of the recombinant protein to assay the motor ac-

tivity in vitro. These data demonstrate the importance of motion in the reactive sulfhydryl region and identify G699 as a likely pivot point.

Materials and Methods

Expression Vector Construction

Skeletal muscle myosin expression vectors were constructed from a full-length chicken embryonic fast skeletal muscle myosin heavy chain cDNA that was isolated from a 14-d in ovo pectoralis major cDNA library (Molina et al., 1987). A chimeric chicken myosin cDNA was created by replacing the 5'-segment of the embryonic myosin cDNA with the corresponding segment from an adult pectoralis muscle myosin gene (Robbins et al., 1986). This was done to incorporate the adult segment that encodes amino acid residues 1–60 of the myosin protein sequence and contains three unique epitopes recognized by mAbs (Winkelman et al., 1993). A plasmid containing a rat embryonic myosin heavy chain minigene (pE2600) was kindly provided by Dr. Vijak Mahdavi (Harvard Medical School, Boston, MA). This plasmid contains the complete embryonic rat skeletal muscle myosin promoter/enhancer region (1.4 kbp), the first two exons, a large deletion fusing the third exon to the 37th exon, and the last four exons (38–41) of the rat myosin gene (Bouvagnet et al., 1987). The selection vector, pSV2Neo, was a gift from Dr. Jean Schwarzbauer (Princeton University, Princeton, NJ). This plasmid contains a neomycin phosphotransferase gene linked to the SV-40 early promoter region and SV-40 late sequences that contain splicing and polyadenylation signals (Southern and Berg, 1982).

To construct the 5'-end of the expression vector, a 1.67-kbp HindIII–BamHI fragment containing the complete promoter/enhancer region of the rat myosin gene and a 0.56-kbp BamHI–Cfr10I fragment containing exons 1–2 were isolated from pE2600. Synthetic oligonucleotides corresponding to a 22 mer (CAT GGT GTT GGC CTG AGT CAC A) and a 26 mer (CCG GTG TGA CTC AGG CCA ACA CCA TG) were synthesized (Operon Technologies, Inc., Alameda, CA), annealed, and phosphorylated to obtain a Cfr10I–NcoI blunt end linker for introducing a translation start site and unique NcoI cloning site at the 3'-end of the second exon of the rat myosin gene. The 1.67-kbp HindIII–BamHI fragment, 0.56-kbp BamHI–Cfr10I fragment, and Cfr10I–NcoI blunt linker were cloned into the HindIII–SmaI sites of pGEM3 (Promega Corp., Madison, WI). The resulting intermediate plasmid contains the complete promoter and first two exons of the embryonic rat myosin gene with a unique NcoI restriction site for the insertion of chicken myosin cDNAs.

The 3'-end of the rat myosin gene corresponding to exons 37–41 is contained in a 1.93-kbp PstI–EcoRI fragment of pE2600. The PstI site is shared between rat and embryonic chicken myosin cDNAs. A 365-bp NcoI–PstI fragment from the embryonic chicken myosin cDNA corresponding to exon 37 of the rat myosin gene was ligated together with the PstI–EcoRI fragment into the NcoI–EcoRI sites of the intermediate plasmid. Together, the 5'- and 3'-ends of the rat myosin gene complete the shuttle vector pGrM. The construction was confirmed by restriction mapping and sequencing across all junctions. The embryonic chicken myosin heavy chain cDNA was cloned between the NcoI site and a unique XhoI site in the pGrM vector. The resulting vector was designated pGrMHC.

Site-directed Mutagenesis

PCR was used to introduce base changes within the myosin cDNA. The primer, TCC GGA TCC CTT CCA GCA CGG CGT TAC, overlaps the codon for G699 and was designed to insert two single base changes: one change converted the glycine codon to an alanine codon, and the other change, 18 bases away, is a silent mutation that introduces a unique BamHI restriction site. This antisense strand primer was paired with an upstream primer overlapping a unique BglII restriction site to produce a 740-bp PCR product. A second sense strand primer, GGA AGG GAT CCG GAT TTG C, also containing the silent mutation for the unique BamHI site, was paired with a unique downstream primer overlapping a ClaI cloning site to produce a 320-bp PCR product. The two PCR products were completely sequenced; then the mutagenized region was inserted into the pGrMHC plasmid to yield pGrMHC/G699A.

Cell Culture and Transfections

The myogenic cell line, C2C12 (ATCC CRL 1772), was purchased from American Type Culture Collection (Rockville, MD). This is a mouse myo-

genic cell line derived by serial passage of primary cultures of adult thigh muscle after injury (Yaffe and Saxel, 1977). For routine passage, C2C12 myoblasts were plated at 2×10^3 cells per cm^2 and maintained in 10% FBS, 90% DME (GIBCO BRL, Gaithersburg, MD) at 37°C in 5% CO_2 (Moncman et al., 1993). The cells were passed every 2–3 d when 60–70% confluent. For formation of C2 myotubes, the cells were transferred to differentiation media (10% horse serum, 1% FBS, 89% DME) as they reached confluence. The cells line up and fuse into multinucleated myotubes.

Primary cultures of chicken embryonic breast muscle were prepared by dissection of d11 embryos and enzymatic dissociation of the tissue. The cultures were maintained in 10% FBS, 90% DME/F12 medium (Sigma Chemical Co., St. Louis, MO). The breast muscle from two embryos was removed, rinsed in PBS, minced with a scalpel in 2 ml of PBS, and vortexed for 30 s. 2 ml of 0.25% trypsin in PBS was added to the tissue and incubated at 24°C for 10–20 min. The tissue was collected by centrifugation in a clinical centrifuge for 5 min at 1,000 rpm and washed with 10% FBS, 90% DME/F12. The cells were then dispersed by treatment with 2,000 U of collagenase in 10 ml of DME for 2 h at 37°C with gentle pipetting every half hour. Large tissue clumps were removed by filtering the cells through a nylon membrane. The cells were collected, washed with 10% FBS, 90% DME/F12, and plated at 6×10^3 cells per cm^2 . The media were changed every other day, and the cells differentiated as they approached confluence.

Stable transfection of C2C12 cells was performed using a liposome-mediated procedure with Lipofectin (GIBCO BRL) according to the manufacturer's recommendations, but optimized for use with the C2C12 cell line as previously described (Moncman et al., 1993). C2 myoblasts were plated at 6×10^3 cells per cm^2 in 6-well cluster plates and grown at 37°C for 24 h (cells were 50–60% confluent at the time of transfection). For transfections, 5 μg of DNA and 35 μg of Lipofectin were mixed and added. After incubation at 37°C for 5 h, the transfection was stopped by dilution with 3 ml of 20% FBS in DME. For most transfections the molar ratio of myosin gene to selection vector (pSV2Neo) was 50:1.

The transfected cells were split into medium containing 1 mg/ml G418 (Geneticin; Life Technologies, Inc., Gaithersburg, MD) and plated in a 100-mm culture dish 36–48 h after transfection. The selection media was changed every 3 d to remove debris. Isolated colonies were visible 7–10 d after transfection. Colonies were picked using a filter lift trypsinization method (Domann and Martinez, 1995). The filters were transferred to a 24-well cluster plate and expanded to larger plates as they reached 50–60% confluence. Isolated clonal lines were induced to fuse, and the myotubes were assayed for myosin expression by Western blot assay. Lines that tested positive for expression of the myosin gene were expanded, frozen at -80°C , and stored in liquid nitrogen.

PCR Amplification

Genomic DNA was prepared from 80–100% confluent 100-mm plates of C2 cell lines using standard procedures (Sambrook et al., 1990). Amplification of the genomic DNA (100 ng) with the PCR was for 30 cycles of 94°C for 30 s, 58°C for 30 s, and 72°C for 30 s with 1- μM primers, CTG GAC ATC GCT GGC TTT G and TTC TCT TGC AGC AGG GAC ACC, using Taq polymerase (Boehringer Mannheim GmbH, Mannheim, Germany). The primers were selected to flank the region encoding the G699A point mutation and to produce a 1.28-kbp amplified product. Total RNA was isolated using TRIzol Reagent (Life Technologies, Inc.) according to the manufacturer's recommendations. The cDNA was synthesized from 500 ng of total RNA primed with random hexamers using M-MLV reverse transcriptase (RT)¹ (Life Technologies, Inc.). Primers used for PCR amplification were designed to overlap splice junctions on the 5'- and the 3'-end of the processed myosin mRNA. The primers for RT-PCR of the 5'-end of the mRNA were: CTG CCA CAG TCA GAG GTC CC (position 10–29) and GCT CCA GGC TGT TGA AAT C (position 1526–1508). The primers' 3'-end of the RNA were: GCT GAG CCA TGC CAA CCG CCA G (position 4993–5014) and GCA TGT GGA AAG GGG TTA CGT GG (position 6027–6005). Amplification of the cDNA (100 ng) with 1- μM primers using Taq polymerase was for 30 cycles consisting of 94°C for 30 s, 60°C for 30 s, and 72°C for 30 s. PCR products were analyzed by Tris-acetate EDTA agarose gel electrophoresis (Sambrook et al., 1990).

1. Abbreviations used in this paper: F-actin, filamentous actin; RT, reverse transcriptase.

Monoclonal Antibodies

A library of mAbs that react with skeletal muscle myosin heavy chain was prepared and characterized as previously described (Winkelmann et al., 1983, 1993, 1995; Winkelmann and Lowey, 1986). The IgG class mAbs were purified on protein A–Sepharose from ascites fluid obtained by passage of hybridoma lines through CAF1/J mice (Winkelmann et al., 1983). All of the antibodies used in this study were extensively characterized for their patterns of cross-reactivity with myosin from different developmental stages and species (Moncman, 1993). mAbs were conjugated with FITC, rhodamine isothiocyanate, or biotin as previously described (Moncman et al., 1993). For immunofluorescence microscopy, cells were grown on glass coverslips that were coated with 0.1–0.5% porcine gelatin (Sigma Chemical Co.) and processed as previously described (Moncman et al., 1993).

Isolation of Myosin from C2 Myotubes

Confluent C2 myoblasts were switched to fusion media, and the differentiated myotubes were processed 6–10 d later. The cell layer was rinsed twice with 5–10 ml cold PBS. Then 1 ml of Triton extraction buffer (TEB: 0.5% Triton X-100, 150 mM NaCl, 10 mM Imidazole, pH 7.0, 0.2 mM PMSF, 1.0 mM DTT) was added per 100-mm plate, and the cell layer was scraped and transferred to a Dounce homogenizer (Kontes Glass Co., Vineland, NJ). Each plate was rinsed with an additional 1 ml of TEB, and the rinse was transferred to the next plate. The cell suspension was homogenized 10–15 strokes on ice, and then pelleted for 10 min at 10,000 g at 4°C. The cell pellet was washed twice with TEB and repelleted. The Triton-insoluble fraction was extracted with a small volume (~ 0.5 ml per plates) of high salt buffer (HSB: 0.5 M KCl, 5 mM MgCl_2 , 5 mM Tris-HCl, pH 8.0, 1 mM DTT, 0.2 mM PMSF) with 5 mM neutralized ATP added. The pellet was resuspended by gentle homogenization, and then incubated on ice for 15 min with occasional gentle mixing. The cell debris was pelleted at 10,000 g for 10 min at 4°C. The high salt soluble extract was dialyzed against 1/10 diluted high salt buffer without ATP at 4°C overnight (>16 h). The actomyosin pellet was collected by centrifugation at 10,000 g for 10 min at 4°C and resuspended in a minimal volume of HSB (25 mM Imidazole, pH 7.6, 0.3 M KCl, 4 mM MgCl_2) supplemented with 1 mM ATP. The filamentous actin (F-actin) was pelleted at 90,000 rpm for 21 min in a rotor (TLA 100.2; Beckman Instruments, Inc., Palo Alto, CA) at 4°C, and the myosin-containing supernatant was recovered. Further purification by ion-exchange chromatography on a Mono Q HR5/5 column (Pharmacia Fine Chemicals, Piscataway, NJ) was done after dialysis into 40 mM sodium pyrophosphate, pH 7.5, 1 mM DTT. The myosin was eluted with a linear 0–0.5 M NaCl gradient in the pyrophosphate buffer.

Antibody Capture and Motility Assays

Preparation of the antibody capture surfaces for motility assays has been described in detail (Winkelmann et al., 1995). Briefly, mAb 10F12.3 was bound to nitrocellulose-coated glass coverslips by incubation with 150 $\mu\text{g}/\text{ml}$ mAb in PBS or Imidazole-buffered saline for 15 min at 24°C. The antibody-coated surface was blocked with 1% BSA for 15 min, transferred to myosin diluted in HSB supplemented with 1% BSA (HSB/BSA), and incubated 2–4 h in a humidified chamber at 4°C. The coverslips were washed twice by transferring to 150 μl of HSB/BSA for 5 min per wash, and then rinsed twice by transferring to a 150- μl drop of motility buffer (25 mM Imidazole, 25 mM KCl, 4 mM MgCl_2 , 0.2 mM CaCl_2 , 5 mM 2-mercaptoethanol, 1 mM ATP, pH 7.6) for 30–60 s. The excess motility buffer was wicked off, and the coverslip mounted on 20 μl of 1–3 nM phalloidin-labeled F-actin on a small parafilm ring affixed to an alumina slide with vacuum grease.

Phalloidin-rhodamine-labeled actin was diluted with motility buffer supplemented with 0.5% 2-mercaptoethanol, 0.1 mg/ml glucose oxidase, 0.018 mg/ml catalase, and 2.3 mg/ml glucose to reduce photooxidation (Kishino and Yanagida, 1988). In all assays the MgATP concentration was increased to 7.5 mM, and 0.5% methyl cellulose (1,500 centipoises per 2% aqueous solution; Sigma Chemical Co.) was included. This chamber was observed with a $\times 100$ plan apochromat (1.3 NA) objective on a microscope (BH-2; Olympus Corp. of America, New Hyde Park, NY) equipped with epifluorescence optics illuminated with a 100 W mercury light source and rhodamine filter set. Images were projected with a $\times 3.3$ TV tube onto the photocathode of a microchannel plate image intensifier (Hamamatsu Photonics, Bridgewater, NJ) optically coupled to a video camera and recorded with an S-VHS video recorder. The temperature of the alumina slide was maintained at 27°C with a Peltier stage heating/cooling device

(Physitemp Instruments, Clifton, NJ). Movement of actin filaments in the sealed chamber can be observed for >2 h; however, measurements were taken within 30 min of slide preparation.

Motion Analysis

Videotaped motility assay data are analyzed with a semi-automated filament tracking program (Bourdieu et al., 1995). Individual video frames are acquired from a frame accurate VCR (Sanyo GVR-S950; Sanyo Fisher Corp., Compton, CA) and digitized on a workstation (Silicon Graphics, Inc., Mountain View, CA). Each digitized frame is processed by adjusting the intensity and contrast with parabolic corrections, and then applying user-defined threshold and rank-depression filters to separate individual filaments from background and refocus the filaments before binarization. The boundary and coordinates for every filament in each frame are compressed and stored to produce a database containing frame number, position, and shape of the filaments. Video segments from 2–8 min are processed in this manner to produce a data set for a single assay condition. For fast-moving filaments, every frame is analyzed; for very slowly moving filaments, a time-lapse feature is used to vary the sampling from 3–30 frames per s.

The database of defined filaments is analyzed with a separate application to define the connectivity in time of the individual filaments and to assign a label to each filament that can be propagated in time. Limitations in assignment of unique labels have been discussed (Bourdieu et al., 1995). Literally hundreds of filaments can be uniquely identified and tracked with this software. The tracks of individual filaments are derived from the skeletonization of the overlapping filament shapes in successive frames. The directed motion of the filaments is defined by mapping the mean arc-length coordinate of the filament onto the track to produce a time-displacement plot. These plots are analyzed to define the filament velocity. This analysis automatically extracts the movements of many filaments without selection bias. However, stationary filaments and trajectories of <20 frames are routinely discarded, so the resulting probability distributions lack a zero velocity component. The database of digitized filaments can be analyzed in a variety of ways, including the creation of time-lapse averages of any number of successive video frames. This is used to represent the quality of movement over a defined period of time.

ATPases, Myosin Quantitation, Electrophoresis, and Western Analysis

Actin-activated myosin ATPase activity was measured in motility buffer at 30°C with 10 μ M F-actin by measuring phosphate release using the Malachite green assay (Kodama et al., 1986). Myosin samples were immobilized on 12-mm-diam glass coverslips via the antibody capture method, and then floated on 450- μ l drops of assay buffer. Aliquots were withdrawn at intervals, and phosphate content was measured. At the completion of the assay, the coverslip surfaces were washed to remove excess F-actin, and then the bound myosin was eluted with hot 1% SDS sample buffer and analyzed by gel electrophoresis according to Laemmli (1970). Densitometry of the myosin heavy chain region of the stained gel was used to normalize the ATPase activity data. To measure the concentration of recombinant myosin in different preparations, serial dilutions of myosin samples were dot blotted, followed by immunodetection with a recombinant myosin specific mAb (4H7.6) and densitometry. Adult chicken pectoralis myosin contains the identical epitope and was used as the standard in this assay. Electrophoretic transfer of cell extracts to nitrocellulose (BA 83; Schleicher & Schuell, Keene, NH) was done at 6 V/cm for 1 h. Antibody binding to nitrocellulose replicas (Western and dot blots) was detected with HRP-conjugated goat anti-mouse IgG (GIBCO BRL) followed by Luminol chemiluminescence (Pierce Chemical Co., Rockford, IL).

Results

Development of a Muscle Myosin Expression System

We wanted to develop a system capable of producing skeletal muscle myosin for biochemical assays, but also able to assemble muscle-specific filaments. A variety of myogenic cell lines are available that are readily transfected with exogenous genes and are capable of differentiating into myotubes that spontaneously contract. An excellent example is

the mouse myogenic cell line, C2C12 (Yaffe and Saxel, 1977). This cell line has been used extensively to define muscle-specific promoter elements necessary for temporally regulated and tissue-specific expression of muscle genes. For example, the embryonic rat skeletal muscle myosin promoter is active in C2C12 cells and has been extensively characterized in transient transfection assays using reporter gene constructs (Bouvagnet et al., 1987; Moncman, 1993). This promoter was selected to drive the expression of a chicken myosin heavy chain cDNA in C2C12 cells.

We constructed a plasmid, pGrMHC, containing the complete rat embryonic skeletal muscle myosin promoter/enhancer region (1.4 kbp) and the first two noncoding exons of the rat gene, and a chicken myosin cDNA fused in-frame to the 37th exon of the rat gene and including the last four exons (38–41) of the rat myosin gene (Fig. 1 A). In this expression plasmid, the recombinant myosin gene is under the control of a rat myosin promoter and contains splicing signals for processing of the primary transcript to produce a myosin mRNA with native 5' and 3' untranslated regions. The vector was designed to contain unique restriction sites for easy insertion and substitution of segments of the chicken myosin cDNA.

The protein encoded by the recombinant myosin gene is also quite unique (Fig. 1 B). The NH₂ terminus contains the first 60 residues of adult chicken pectoralis muscle myosin, which contains three unique epitopes and was engineered into the gene for easy immunodetection (Winkelman et al., 1993). The next 1760 amino acids of the protein are encoded by the embryonic chicken fast muscle myosin cDNA, and the last 123 amino acids are encoded by exons 37–41 of the embryonic rat myosin gene. Thus, the recombinant gene product is a three-part chimera. The junctions between the different segments of the protein were engineered into conserved regions of the related pro-

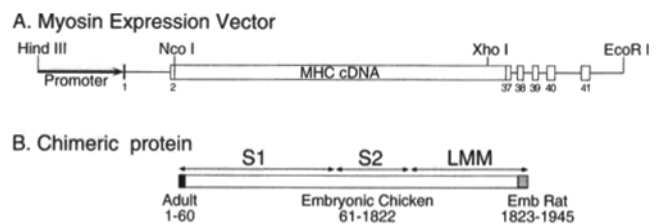


Figure 1. Block diagram of the myosin gene coding region of the shuttle vector that was developed for the stable expression of recombinant myosin in C2C12 cells. (A) The chimeric myosin gene was constructed from segments of an embryonic rat muscle myosin gene (Strehler et al., 1986; Bouvagnet et al., 1987) and contains the promoter/enhancer region, the first two exons, and the last five exons of the rat gene. The chicken myosin cDNA is cloned between the NcoI and XhoI sites shown. The insert depicted here was cloned into the HindIII and EcoRI sites of the vector pGEM3 (Promega Corp.). (B) The myosin heavy chain encoded by the vector contains the first 60 amino acids of an adult fast chicken myosin gene, including three epitopes recognized by species specific mAbs. The bulk of the protein (residues 61–1,822) is encoded by an embryonic chicken fast myosin cDNA. The last 123 residues are contributed by the last five exons of the embryonic rat myosin gene, as is the 3'-untranslated region of the myosin mRNA. The vector has been engineered to facilitate manipulation of embryonic chicken muscle myosin cDNAs.

teins and do not introduce disruptions in the respective domains.

Recombinant myosin genes were introduced into the C2C12 myogenic cell line by cotransfection with a selection vector containing a drug resistance marker (pSV2 Neo) using a liposome-mediated transfection protocol (Moncman et al., 1993). One gene encoded the recombinant chimeric myosin and, for simplicity, is referred to as "wild-type" myosin gene. The other gene containing a glycine to alanine mutation at residue 699 (G699A) of the myosin S1 structure is referred to as "G699A mutant" myosin gene. Individual drug-resistant colonies were screened for expression of the recombinant myosin. The rat myosin promoter is only active when the myoblasts withdraw from the cell cycle, align, and fuse during differentiation. Transfected C2C12 colonies were induced to differentiate, and after 6 d, most of the clones had formed multinucleated myotubes. A crude cytoskeleton fraction was prepared from the undifferentiated myoblasts and 6-d-old myotubes, and this fraction was screened for the recombinant myosin by SDS-PAGE and Western blotting (Fig. 2). The differentiation of the C2 clones is marked by a large increase in the expression of muscle-specific cytoskeletal proteins and, in particular, myosin. This is illustrated for one clone that was transfected with the wild-type recombinant myosin gene and one clone transfected with the G699A mutant myosin gene. The mAb antibody used in this screen is directed against an epitope on the NH₂ terminus of the recombinant myosin and does not cross-react with the endogenous C2 myosin.

The clones were classified both on the level of recombinant myosin expression and on the extent of differentiation. Strongly positive lines exhibiting good differentiation were selected for further analysis. Expression of the re-

combinant myosin is stable over multiple passages; however, the extent and quality of differentiation and the level of expression does decrease with extended passage (through passage 13). Consequently, all experiments were performed with early passages of positive clones.

Recombinant Myosin Expression

The presence of the wild-type and G699A mutant transgenes in transfected C2 cell clones was confirmed by PCR amplification of genomic DNA. Oligonucleotide primers that flanked the position of the G699A point mutation within the myosin coding region were used to amplify the target sequences in genomic DNA isolated from untransfected C2C12 myoblasts, a cell line transfected with the wild-type myosin gene and a line transfected with the G699A mutant myosin gene (Fig. 3 A). A 1,281-bp fragment is detected in both clones that had been selected for expression of the recombinant myosin gene, and no fragment is amplified from the C2C12 myoblasts. In designing the site-directed mutagenesis primers to produce the G699A mutation, an adjacent silent base pair change was incorporated to introduce a unique BamHI restriction site in the coding region of the myosin cDNA. Consequently, when the PCR products from the wild-type and mutant clones were digested with BamHI, the PCR fragment from the mutant was cleaved, producing 736- and 545-bp fragments, confirming the identification of the mutant cell line.

The regulation of the recombinant myosin gene expression and processing of the transcript were analyzed by RT-PCR. A set of primers was designed to analyze splicing on the 5'-end of the mRNA (Fig. 3 B). The (+) strand primer overlapped the putative splice junction between exon 1 and exon 2 of the recombinant gene. The (-) strand primer was selected from within the coding region of the myosin cDNA such that if the first intron were properly excised from the primary transcript, a 1.5-kbp PCR product would result. Total RNA samples from myoblasts and myotubes (6 d after induction) were analyzed by RT-PCR. The predicted 1.5-kbp PCR product is detected only in the cDNA produced with the myotube RNA samples from the cell lines bearing wild-type and mutant myosin genes. This indicates that the recombinant myosin gene is only expressed in differentiating myotubes. The size of the fragment is exactly that predicted, assuming the primary transcript was properly processed. Similarly, primers were designed to analyze the processing of the 3'-end of the recombinant gene transcript using a (+) strand probe in the chicken cDNA near exon 37 and a (-) strand probe in the rat exon 41 (Fig. 3 C). Again the predicted PCR product (1.03 kbp) is detected in the cDNA samples from the differentiated myotubes of the clonal lines expressing the recombinant chicken myosin genes. These results indicate that the recombinant myosin genes are temporally regulated and active only in myotubes and that the primary transcripts are properly processed.

The time course of the appearance of the recombinant myosin in differentiating myotubes was assayed by SDS-PAGE and Western blotting. A clone expressing the wild-type myosin was induced to differentiate, and a high salt extract of the cytoskeletal proteins was harvested at intervals during myotube formation. After transfer to the dif-

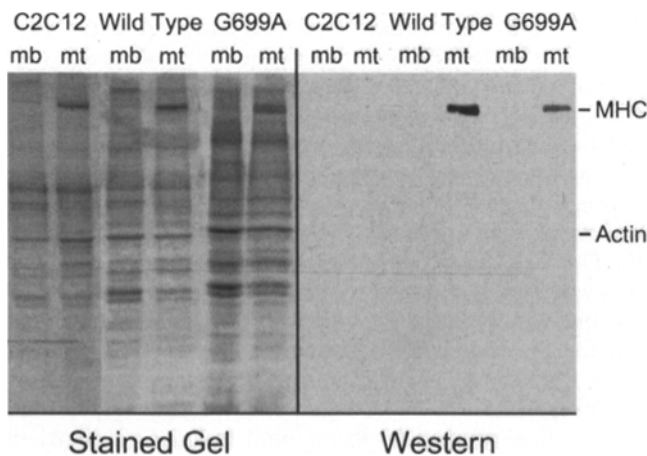
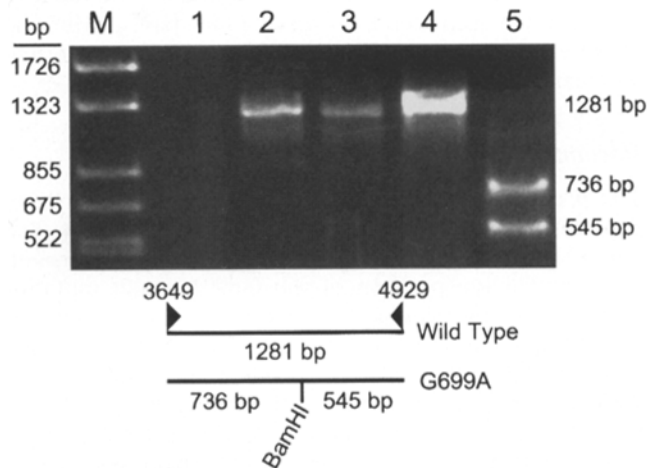
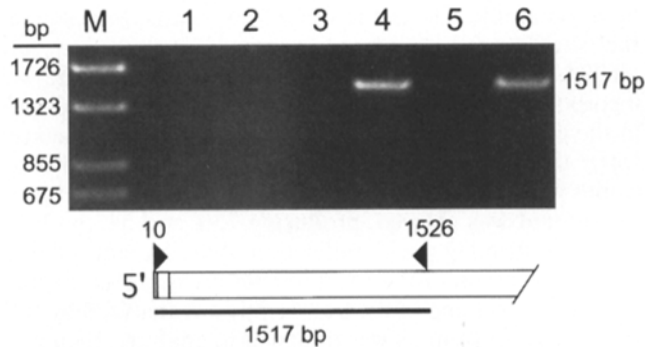


Figure 2. Expression of recombinant myosin in C2C12 transfectants. Stable transfectants were induced to differentiate, and then screened by Western blotting for the production of the recombinant myosin using an mAb (4H7.6) that specifically recognizes the chicken myosin. The analysis of three cell lines is shown: untransfected C2C12 cells (C2C12), and two clones from transfections with the wild-type myosin gene and the G699A mutant myosin gene. Clones isolated with this screen synthesized the recombinant myosin in differentiated myotubes (*mt*) but not in myoblasts (*mb*). The recombinant myosin was detected in 20–60% of the clones that were screened.

A. Genomic PCR



B. 5'RT-PCR



C. 3'RT-PCR

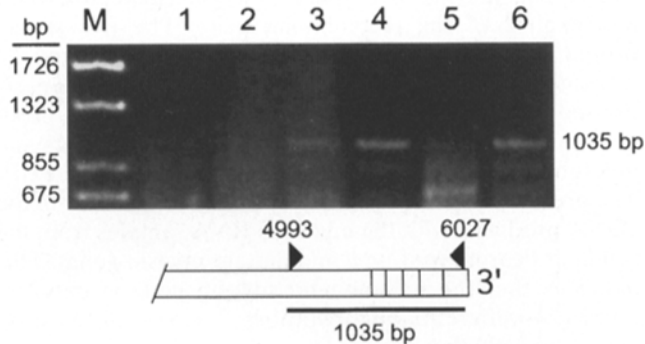


Figure 3. Genomic PCR analysis of wild-type and mutant clones and RT-PCR analysis of recombinant myosin mRNA. (A) Genomic DNA was isolated from C2C12 cells (lane 1) and cell lines expressing wild-type myosin (lanes 2 and 4) and G699A mutant myosin (lanes 3 and 5). Primers that flanked the position of the point mutation (G699A) were selected from the chicken myosin cDNA sequence. PCR amplification using these primers produces the expected 1,281-bp product with the genomic DNA from wild-type and G699A mutant myosin-expressing cell lines, but not C2C12 cells. BamHI restriction enzyme digestion of the wild-type (lane 4) and G699A mutant (lane 5) PCR products produces 735- and 545-bp fragments only with the G699A mutant PCR product. (B and C) RT-PCR of total RNA isolated from myoblasts (lanes 1, 3, and 5) and myotubes (lanes 2, 4, and 6) from C2C12 cells (lanes 1 and 2), a wild-type myosin-expressing clone (lanes 3 and 4), and G699A mutant-expressing clone (lanes 5 and 6). Primers were selected for analyzing the 5'- and the 3'-

differentiation media, the myoblasts quickly begin to align and fuse, and within 48 h, there is a marked increase in the amount of muscle-specific cytoskeletal proteins, most notably myosin (Fig. 4). However, the recombinant myosin is not detected until 4–5 d after induction, at least 48 h after the initial appearance of the muscle-specific C2 myosin and well after significant accumulation of the endogenous myosin. This suggests that the rat promoter driving expression of the recombinant myosin is a late promoter turning on after the initial burst of muscle-specific gene expression. The level of expression of the recombinant myosin appeared stable in the myotubes for up to 14 d (data not shown).

The stability of the recombinant myosin may be accounted for by the observation that this myosin coassembles with the endogenous C2 myosin into the striated myofibrils of the myotubes (Fig. 5). The cloned myoblasts were grown on collagen-coated glass coverslips, induced to differentiate, and processed for immunofluorescence microscopy 6 d after the appearance of myotubes. The recombinant myosin is detected, assembled into well-ordered, striated myofibrils in these myotubes. Both the wild-type myosin (Fig. 5 A) and the G699A mutant myosin (Fig. 5 B) coassemble with the C2 myosin, demonstrating that these genes produce assembly-competent proteins. In addition to striated myofibrils, the protein is found diffusely distributed throughout the myotubes along cytoskeletal structures and in poorly organized myosin filament bundles, sites characteristic of the cytoarchitecture of nascent myotubes.

Isolation of the Recombinant Myosin

Since the recombinant myosin coassembles with the muscle-specific cytoskeleton, it was readily isolated along with the endogenous C2 myosin using typical myosin extraction and fractionation methods (Fig. 6). Myotubes were harvested 7–8 d after fusion, lysed, and extracted with Triton X-100 to remove soluble proteins and to produce a Triton-insoluble cytoskeleton fraction. The myosin was recovered from the cytoskeleton fraction by extraction with a high salt buffer containing ATP. An acto-myosin superprecipitate was then formed by overnight dialysis of the high salt extract against a low salt buffer lacking ATP. The acto-myosin pellet was redissolved in high salt/ATP buffer, and the F-actin pelleted to recover an enriched myosin fraction that was used in most subsequent assays (Fig. 6 A). The recombinant myosin fractionated with the C2 myosin throughout the preparation and amounted to 2–5% of the total myosin fraction. About 20–40 μ g of recombinant myosin was prepared from 0.25–0.5 g of cell pellet.

As a final step, the recombinant myosin was partially separated from the endogenous C2 myosin by ion-exchange

end of the mRNA separately. PCR products of the predicted size (1,517 bp for the 5'-end RT-PCR and 1,035 bp for the 3'-end RT-PCR) are detected on amplification of the cDNA produced from the total RNA. The products are produced only with RNA isolated from myotubes of cell lines expressing the recombinant myosin gene. These results indicate that recombinant myosin gene expression is correctly regulated and that primary transcripts are properly spliced.

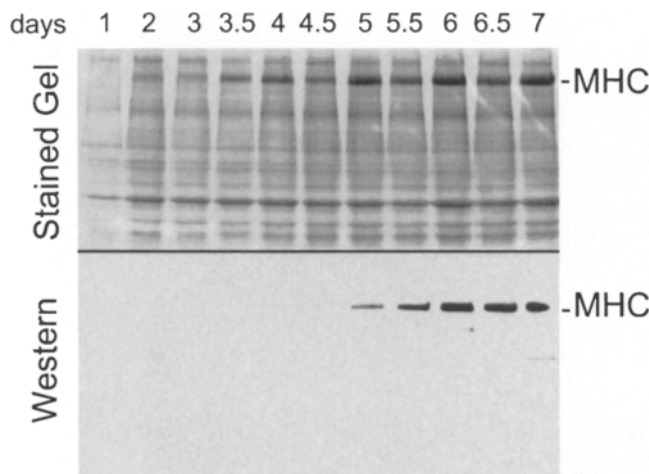


Figure 4. The time course of recombinant myosin expression in developing myotubes. Confluent 100-mm dishes of myoblasts were induced to differentiate by transferring to low serum media. A high salt extract of the Triton-insoluble cytoskeleton was analyzed by SDS-PAGE and Western blotting. Myotubes formed quickly over the course of several days. The extent of differentiation is indicated by the increase in the level of myosin expression, which is apparent in the stained gel. Myosin synthesis increases from day 2 to day 7; however, the recombinant myosin is not detected until 4.5–5 d after induction, suggesting that the rat myosin promoter is a late promoter, turning on after the initial induction of the muscle-specific gene expression program.

chromatography (Fig. 6 B). The recombinant myosin elutes in the leading edge of the myosin peak as shown by Western blotting. The recombinant myosin and the C2 myosin elute with the muscle-specific myosin light chains: emb-LC1, LC1, LC2, and a small amount of LC3. This indicates that the recombinant myosin is a chimeric protein containing mouse muscle-specific light chains associated with chicken myosin heavy chain sequences. Despite this unusual combination, the recombinant myosin has assembly and solubility properties that are comparable to the embryonic mouse myosin.

Motor Activity of Recombinant Myosin

Expression of both the recombinant myosin and the endogenous C2 myosin are induced during myoblast differentiation. Therefore, it was necessary to devise an approach that could isolate the recombinant myosin from the C2 myosin to selectively assay the motor activity of the recombinant protein. This was accomplished using an antibody capture technique to prepare surfaces for *in vitro* motility assays (Winkelman et al., 1995). An anti-S2 mAb (10F12.3) that reacts with the chicken myosin but not with the C2 myosin was used to selectively tether the recombinant myosin to antibody-coated glass coverslips. The antibody binds the myosin in the S2 region near the S2–light meromyosin junction, leaving the motor domains and much of the S2 region free to interact with actin and to power the sliding movement of actin filaments. This is a very sensitive method for specifically isolating myosin from dilute mixtures and has been demonstrated to produce surfaces that support rapid and uniform sliding movement of actin filaments at speeds that approach the unloaded

shortening velocity measured for muscle contraction (Winkelman et al., 1995).

The myosin fractions isolated from wild-type and G699A mutant myosin-expressing clones, a native myosin isolated from adult chicken pectoralis muscle that also reacts with the anti-S2 mAb and C2 myosin isolated from an untransfected cell line, were incubated with the anti-S2-coated coverslips. The sliding movement of fluorescently labeled actin filaments over these surfaces was recorded by video microscopy and analyzed. The type of movement that is observed is illustrated in Fig. 7, which shows the accumulation of tracks produced by single actin filaments as they move over each of these surfaces. Large numbers of individual tracks are apparent, crisscrossing the field over the adult chicken myosin (Fig. 7 A) and recombinant wild-type myosin (Fig. 7 B) in the 2-min time windows displayed here. Individual actin filaments move smoothly onto the myosin-coated surfaces from the bulk solution and often transit over distances of several hundred microns. A few immobilized actin filaments are also apparent, as evidenced by the bright spots, but most of the field is dominated by filament tracks. The appearance of the tracks is markedly different for the G699A mutant myosin (Fig. 7 C). These tracks were accumulated over 6 min and appear much brighter, shorter, and more heavily curved. This is because the actin filaments making these tracks were moving exceptionally slowly over this myosin-coated surface.

In contrast to the directed and active movement as evidenced by the numerous tracks produced over the adult and recombinant myosin-coated surfaces, the surface incubated with C2 myosin supports no directed movement and produces no long actin movement tracks (Fig. 7 D). The actin filaments near the surface gyrated in Brownian motion, producing a few short branched tracks and circles; however, there was no evidence for binding of filaments to the surface or directed movement over the surface in this 2-min time window or in any of the video recordings. This result confirms the selectivity of the antibody capture technique used here.

Movement of the actin filaments was analyzed with a semi-automated tracking program (Bourdieu et al., 1995) to determine the actin filament velocity distributions for adult chicken myosin, wild-type recombinant myosin, and G699A mutant myosin (Fig. 8). This analysis first involves the delineation of all actin filaments in each video frame, followed by frame-to-frame mapping to define the connectivity in time and to assign a label to each filament. The labeled filaments are then propagated through time, and their shape, time, and position coordinates are stored. The track for an individual filament is defined by skeletonization of the superimposed shapes for all frames over which the filament has been followed. Hundreds of these tracks have been extracted from several minutes of video recording for each of the myosin surfaces analyzed. Several tracks are shown for filaments moving over the wild-type myosin (Fig. 8 A) and the G699A mutant myosin (Fig. 8 B). The average track duration for the wild-type myosin was ~10 s during which the filaments traveled ~35 microns. There is a marked difference in the length and duration of the tracks extracted for filaments moving over the G699A myosin-coated surfaces. Individual filaments moved

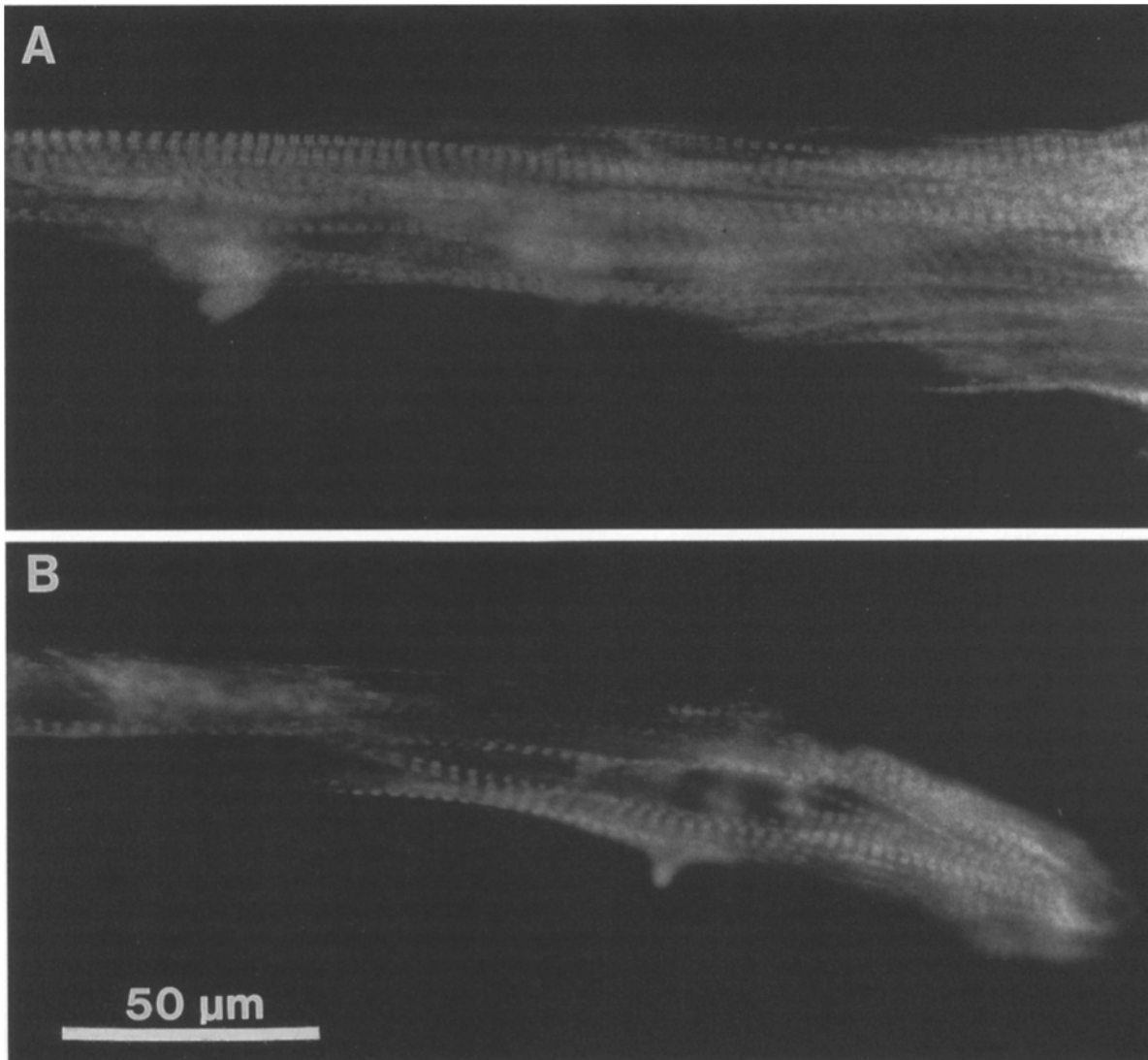


Figure 5. Immunofluorescence analysis of recombinant myosin assembly in stable clones. The recombinant myosins were detected with a rhodamine-conjugated mAb that specifically recognizes the NH₂-terminal region of the protein (12C5.3). The recombinant myosins assemble into highly ordered, striated myofibrils in C2 myotubes derived from cloned myoblasts. (A) Immunofluorescence microscopy of multinucleated myotubes formed from a clone expressing the wild-type recombinant myosin. The chicken myosin coassembles with the endogenous C2 myosin into striated myofibrils spanning the entire length of this myotube. (B) Similarly, the G699A mutant myosin is found assembled in striated myofibrils.

very slowly over this myosin, so slowly that they could be tracked for as long as 5 min, during which they traveled only a few microns. The limiting factor for tracking these filaments was photobleaching. Most of the filaments moved persistently over the entire observation period; however, the motion was perceptible only as changes in filament shape or if the video records were fast-forwarded.

To determine the velocity of movement, the mean arc length coordinates of the filament in each frame is projected onto the track to produce a time-displacement plot with the slope equivalent to the instantaneous velocity of the filament moving along the track. Several such time-displacement plots are shown for filaments moving over wild-type myosin (Fig. 8 C) and G699A myosin-coated surfaces (Fig. 8 D). The predominant motion observed over the wild-type myosin is smooth gliding movement of the actin

filaments occasionally interrupted by short stalls. This is very much like the movement that has been described in detail for adult myosin (Bourdieu et al., 1995; Winkelmann et al., 1995). The time-displacement curves show periods of motion with similar slope (velocity) interrupted by very short horizontal segments during which the filaments creep along. Filaments moving over the G699A mutant myosin produced time-displacement curves that reveal persistent motion for hundreds of seconds but covering much shorter total distances.

To compute the mean velocity, the experimental curves are broken into a limited number of line segments, and the instantaneous velocity for each segment is weighted by the duration of the segment and plotted as a probability distribution. The mean velocity for the wild-type myosin is 3.4 μm/s, somewhat slower than the 5.5 μm/s measured for

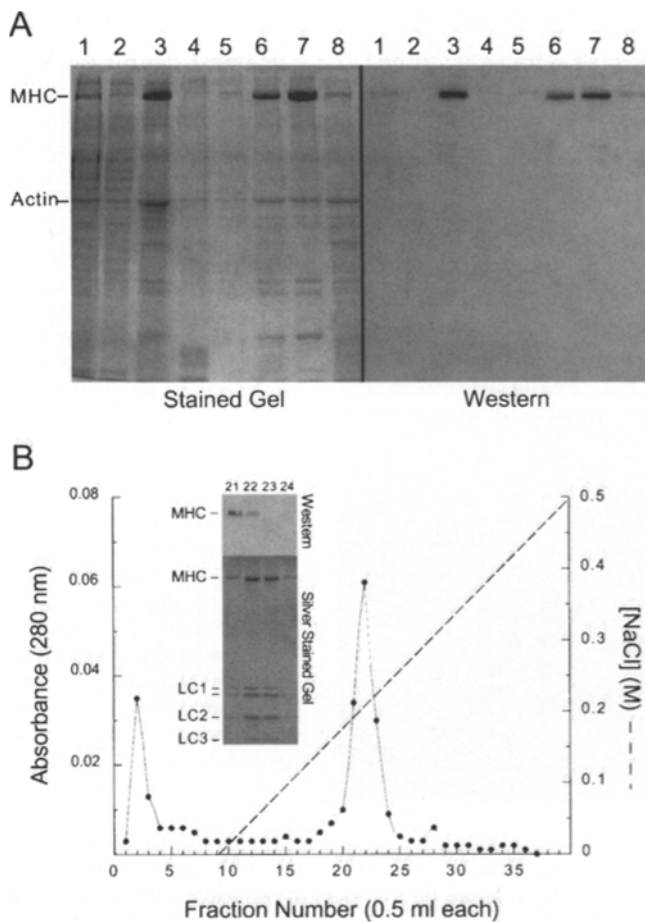


Figure 6. Isolation of the recombinant myosin from myotubes. (A) Isolation of myosin from C2 myotubes analyzed by SDS-PAGE and Western blotting. Samples are: (lane 1) whole cell lysate; (lane 2) lysis supernatant; (lane 3) high salt/ATP extract of Triton-insoluble cytoskeleton; (lane 4) high salt-insoluble material; (lane 5) supernatant from low salt precipitation; (lane 6) acto-myosin superprecipitate redissolved in HSB with ATP; (lane 7) myosin supernatant after high speed centrifugation to pellet F-actin; and (lane 8) F-actin pellet. The recombinant myosin cofractionates with the endogenous C2 myosin and is readily isolated as a mixture with the C2 myosin. The myosin released with MgATP from a superprecipitate with actin (lane 7) was used for most subsequent experiments. (B) The myosin sample (lane 7) was purified by ion-exchange chromatography on a Mono Q column in sodium pyrophosphate buffer. The recombinant myosin elutes in the leading edge of the myosin protein peak as shown by Western blotting (inset). The silver-stained gel reveals the muscle-specific light chains associated with the recombinant myosin. The slower migrating of the two LC1 bands is the embryonic form of this light chain. The recombinant myosin has a complete complement of muscle-specific light chains.

the adult myosin (Fig. 8 E). The mean velocity for filaments moving over the G699A myosin is 0.024 $\mu\text{m/s}$ (Fig. 8 F), over two orders of magnitude slower than the wild-type myosin. Introduction of the G699A point mutation has a dramatic effect on the motor activity of this myosin. Nonetheless, the mutant myosin supports sliding movement of actin filaments that is persistent, and the tight association of the filaments with the surface suggests that the

defect is not related to the number of active motors available on the surface.

The motor domain of the wild-type myosin is derived from the chicken gene, which is expressed in early embryonic breast muscle (Molina et al., 1987). The velocity of actin filament movement produced by the recombinant wild-type myosin ($3.4 \pm 0.9 \mu\text{m/s}$) is similar to that measured for the embryonic myosin isolated either from primary culture myotubes ($3.1 \pm 1.3 \mu\text{m/s}$) prepared from d11 embryo myoblasts or embryonic breast muscle myosin ($3.8 \pm 0.9 \mu\text{m/s}$) isolated from d15 chick embryos. The embryonic myosin samples move actin at $\sim 50\text{--}60\%$ of the velocity of the adult pectoralis muscle myosin, consistent with previous reports (Lowey et al., 1993a).

Functional Significance of the G699A Mutation

The dramatic effect of the G699A point mutation on filament velocity could result from a large decrease in ATPase activity. The actin-activated ATPase activity of the wild-type myosin, G699A mutant myosin, and adult myosin were compared in a solid phase assay. The myosin samples were bound to antibody-coated glass coverslips, and the coverslips were incubated with 10 μM F-actin at 30°C. The phosphate released from Mg-ATP was measured, and the relative activity of the different myosin samples is listed in Table I. The wild-type myosin ATPase activity was slightly lower than that of the control adult myosin, and the G699A mutant myosin was fivefold lower. The fivefold difference in actin-activated ATPase activity between the mutant and either the wild-type or adult myosin is significantly less than expected given the $>100\text{-fold}$ difference in actin filament velocity in the motility assay. This suggests that the predominant effect of G699A mutation on the motor activity of myosin is not the rate-limiting transition that determines the total cycle time and the maximum rate of ATP hydrolysis.

The surface density of active motors is an important factor in determining the velocity of actin filament movement. Above a critical myosin surface density, the actin filament velocity saturates at a maximum. That density is reached with the antibody capture surfaces using $\sim 4 \mu\text{g/ml}$ of the adult myosin (Winkelmann et al., 1995). Below this myosin concentration, there is a marked decrease in filament velocity until movement stops altogether at very low surface densities. The myosin concentration dependence of the actin filament velocity was measured for the wild-type and G699A mutant myosin (Fig. 9 A). The velocity saturates at 3.4 $\mu\text{m/s}$ with the wild-type myosin above 4 $\mu\text{g/ml}$, and below this concentration, the velocity begins to decrease similar to the behavior of adult myosin. This contrasts with the G699A mutant myosin that moves the filaments with a velocity of 0.024 $\mu\text{m/s}$ over the entire myosin concentration range tested (1–10 $\mu\text{g/ml}$). The G699A mutant myosin can support movement at lower myosin surface densities than wild-type or adult myosin. This would occur if the mutation dramatically slows the rate of release of myosin from actin, thereby extending the fraction of the total ATPase cycle spent in a strong binding interaction with actin.

Both the maximum velocity of muscle contraction and the actin filament velocity in the motility assay are deter-

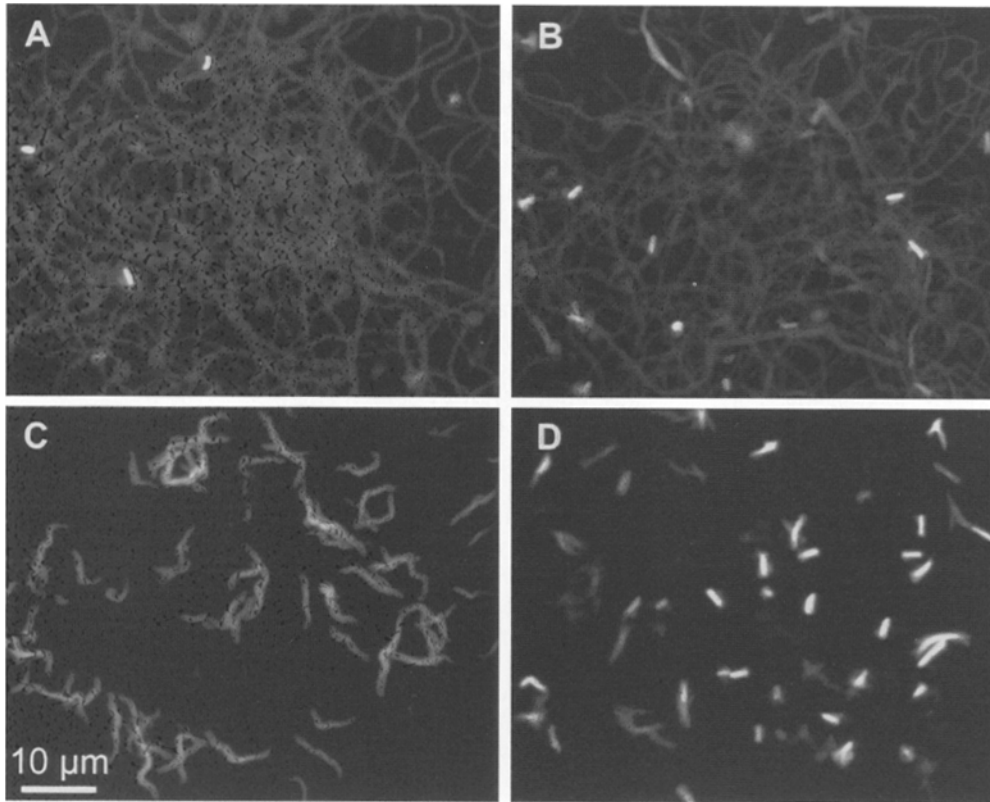


Figure 7. Myosin motor activity assayed with an *in vitro* motility assay. Glass surfaces were coated with an anti-S2 mAb (10F12.3) that reacts with the recombinant myosin but not C2 myosin. This surface was used as an affinity support to separate the recombinant myosin from the C2 myosin and to immobilize the myosin for the motility assay at 27°C. The motor activity of the recombinant myosin is illustrated by the accumulation of actin filament tracks over a myosin saturated surface. (A) Actin filament tracks accumulated over adult chicken pectoralis muscle myosin surface. This myosin was bound by the mAb and demonstrates the normal level of activity observed with this assay during a 2-min accumulation time. (B) The wild-type recombinant myosin supports active movement of actin filaments similar to the adult myosin (2-min accumulation time). (C) The tracks produced

over the G699A mutant myosin-coated surface are brighter, much shorter, and curved. This is due to the slow rate of movement of these filaments (6-min accumulation time). (D) In contrast, C2 myosin supports no directed movement of actin filaments (2-min accumulation time). The filaments observed over this surface do not attach but vibrate in Brownian motion and exhibit no directed movement.

mined by the rate of dissociation of the strongly bound acto-myosin complex at the end of the cycle (Siemankowski et al., 1985). If this step is significantly slower in the G699A mutant, this could explain the greater effect of this mutation on the sliding filament velocity than on the actin-activated ATPase rate. It would also follow that very slowly dissociating G699A mutant crossbridges would interfere with faster cycling crossbridges if both were present in the *in vitro* motility assay. This prediction was tested by preparing surfaces containing a mixture of fast cycling adult myosin with either the wild-type myosin or the G699A mutant myosin (Fig. 9 B). The mixed surfaces were prepared by serial dilution of either G699A myosin or wild-type myosin with a constant concentration of adult myosin (10 μg/ml), and then incubation of the mixtures with antibody capture surfaces. The ratio of adult to wild-type or mutant myosin was varied from 0.5:1 through 125:1. The affinity of the anti-S2 antibody is the same for both the embryonic and adult S2 domains, so the surface density of each motor is proportional to this ratio. Furthermore, at the total myosin concentration used throughout the dilution series, the surface density of motors remains essentially constant (600–700 molecules per μm²), such that velocity of filament movement would be saturated for the adult myosin.

The wild-type myosin had little effect on the velocity of the adult myosin over the entire range tested; this was ex-

pected given the similarity in ATPase activity and actin filament velocity of these two myosin samples. In contrast, the G699A mutant myosin had a dominant negative effect on the filament velocity throughout the range tested. At low ratios of adult myosin to G699A mutant (0.5:1), the filaments were slowed to 0.09 μm/s, a 60-fold decrease in velocity. Even at a 50:1 ratio of adult myosin to mutant myosin, there is still a 50% inhibition of the filament velocity. This indicates that a very small number of slowly cycling G699A mutant crossbridges are sufficient to impose a load on the actin filaments that resists the faster-cycling adult crossbridges. The slow-cycling G699A crossbridges are strongly attached for a significantly longer time than the fast-cycling crossbridges. Thus, the predominant effect of the G699A mutation is on the dissociation of the strongly bound acto-myosin complex at the end of the ATPase cycle.

Discussion

A Muscle Myosin Expression System

We have developed a unique expression system to analyze the effect of site-directed mutagenesis on the motor activity of a skeletal muscle myosin. The regulated expression plasmid, pGrMHC, directs the synthesis of a chimeric muscle myosin in a mouse myogenic cell line and permitted us to manipulate the myosin sequence and subse-

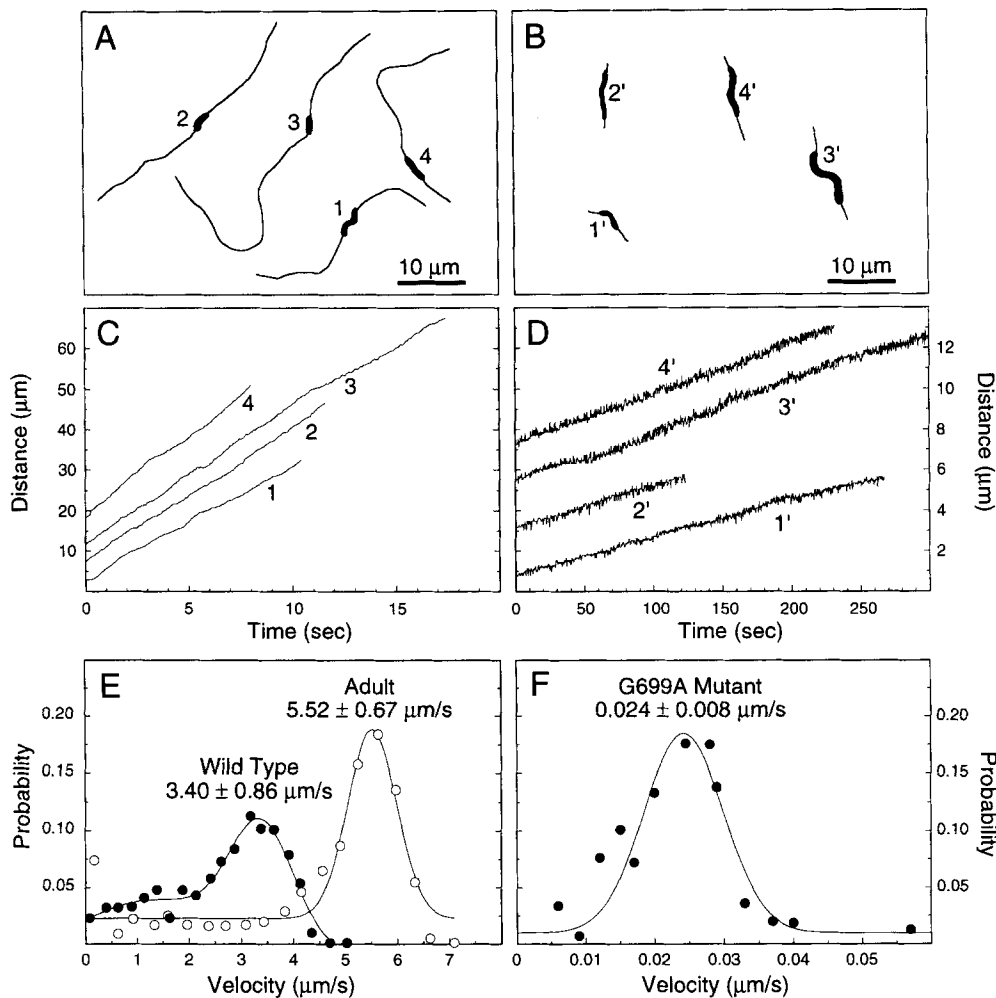


Figure 8. Analysis of motor activity of wild-type myosin and G699A mutant myosin. Movement tracks (A and B), time-displacement plots for selected tracks (C and D), and velocity probability distributions (E and F) are presented for wild-type myosin (A, C, and E) and G699A mutant myosin (B, D, and F). A semi-automated tracking program was used to delineate actin filament tracks. The time-displacement plots corresponding to the selected filaments were produced by projecting the mean arc length coordinate of the filament onto the track for each frame analyzed. Note the difference in the time and distance scales for the wild-type myosin (C) and G699A mutant myosin (D). The duration of the plots for rapidly moving filaments is limited by collisions between filaments. The G699A mutant myosin moved so slowly that collisions were unlikely, thus the duration of movement tracks is 10–30 times longer. The experimental curves are broken into a limited number of line segments to determine the instantaneous velocity (slope of the segment). A velocity distribution is produced by weighting each instantaneous velocity by the duration of the segment. (E and F) Hundreds of observations are binned and plotted as a probability distribution, and the mean velocity is determined by fitting the data to a Gaussian distribution. All motility assays were done at 27°C.

duced by weighting each instantaneous velocity by the duration of the segment. (E and F) Hundreds of observations are binned and plotted as a probability distribution, and the mean velocity is determined by fitting the data to a Gaussian distribution. All motility assays were done at 27°C.

quently isolate and analyze the recombinant protein. The C2C12 cell line was selected because it efficiently produces the muscle-specific isoform of myosin in relatively large amounts and is readily transfected and cloned (Moncman et al., 1993). The development of a regulated expression vector was essential because the constitutive expression

of the same muscle-specific myosin has been shown to interfere with the differentiation of C2 myoblasts (Moncman et al., 1993). This suggested that the coordinate expression of other myofibrillar components is a prerequisite for the proper assembly of myosin and maturation of the muscle-specific phenotype.

Table I. Actin-activated Myosin ATPase Activity

Sample	nmol/mg min (n = 4)
Adult myosin	211 ± 56
Wild-type myosin	188 ± 53
G699A mutant myosin	41 ± 6
Actin alone	0

Actin-activated myosin ATPase activity measured by incubating myosin-coated surfaces with 10 μM F-actin in motility assay buffer at 30°C. Released inorganic phosphate from ATP hydrolysis was quantitated with malachite green assay (Kodama et al., 1986). Background activity measured with actin alone was below the detection sensitivity, as was the Mg-ATPase activity of the myosin surfaces. Activity data were normalized to the amount of myosin bound on the surfaces, which was quantitated by densitometry of the myosin heavy chain separated by SDS-PAGE after eluting the myosin from the surface with SDS sample buffer.

The embryonic rat myosin promoter was used as the basis for building the expression vector. This promoter has been extensively characterized in the C2 myogenic cell line, and is temporally regulated and very active (Bouvagnet et al., 1987; Moncman, 1993). The design was predicated on the desire to include both the 5' and 3' untranslated regions of the rat myosin gene, such that rodent-specific regulatory sequences would drive the expression of the embryonic chicken myosin. The embryonic chicken myosin cDNA was used to take advantage of a library of mAbs, and in particular, an anti-S2 antibody (10F12.3) that made it possible to selectively isolate and assay the recombinant myosin (Winkelmann et al., 1995). The motor domain of this myosin is >95% identical to the adult chicken myosin motor domain, so comparison to the known structure was

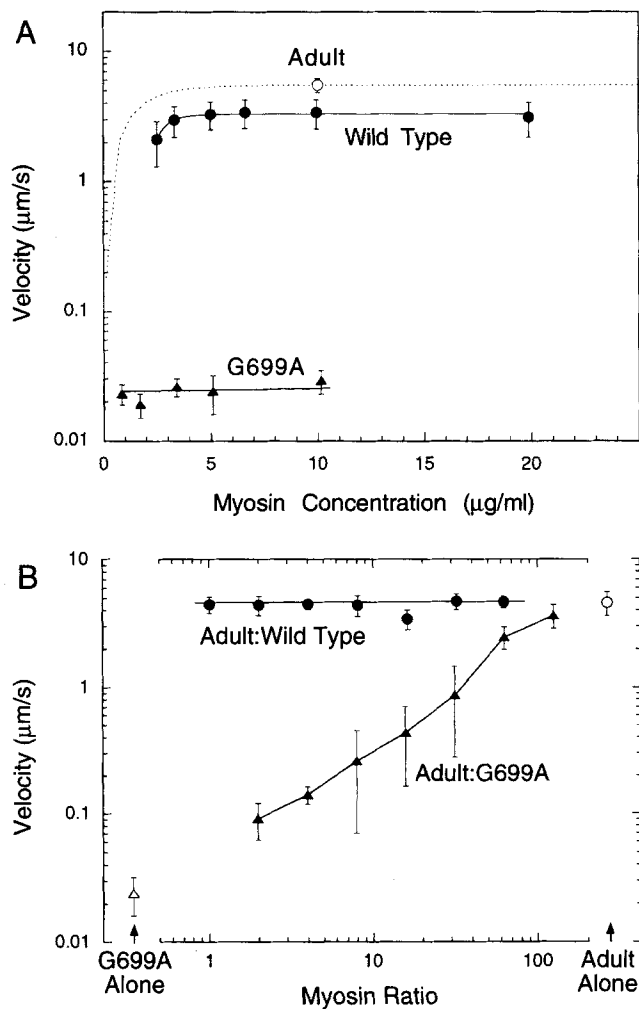


Figure 9. Myosin concentration dependence of the actin filament velocity and interaction between motors. (A) The actin filament velocity was measured on antibody capture surfaces incubated with various myosin concentrations. The dotted line is the concentration dependence measured for adult chicken pectoralis muscle myosin (Winkelmann et al., 1995). The velocity measured for the wild type myosin (●) is constant above 4 µg/ml; however, at lower concentrations, the velocity decreases similar to the behavior of adult myosin. In contrast, the filament velocity powered by G699A mutant myosin (▲) is constant even below the 2 µg/ml threshold. (B) Actin filament velocity measured for mixtures of adult myosin with varying amounts of recombinant myosin. Surfaces were prepared using the antibody capture technique with mixtures of a constant concentration of adult myosin (10 µg/ml) containing varying amounts of wild-type recombinant myosin (●) or G699A mutant myosin (▲). The wild-type myosin has little effect on the adult myosin over the entire range tested. In contrast, the G699A mutant myosin slows the velocities produced by the mixture over the entire range. The velocity of actin filaments moving over the adult myosin alone was 4.6 µm/s (○), and over the G699A myosin alone, it was 0.024 µm/s (△) in these motility assays at 27°C.

another important consideration. Analysis of the expression of the recombinant myosin gene indicates that it is properly regulated and the primary transcript is correctly processed. The time course of expression suggests that the rat promoter is active after the first wave of muscle-spe-

cific gene expression. The low yield of recombinant myosin is perhaps related to the late activation of the promoter. Developmental progression of myosin gene expression in C2C12 cells has been reported (Silberstein et al., 1986), and conditions that favor this progression may be useful for increasing the yield of recombinant myosin from this expression system.

The recombinant myosin is functionally very similar to the endogenous mouse muscle myosin. It coassembles with the mouse myosin light chains that are homologous to the corresponding chicken fast myosin light chain. Both the wild-type and the mutant chimeric myosin are integrated into striated myofibrils and copurify with the endogenous mouse myosin. The phenotypic changes that occurred when recombinant embryonic chicken myosin was expressed constitutively from a viral promoter in C2 cell lines are not evident in these cell lines, indicating that expression of this myosin does not interfere with early or late stages of differentiation (Moncman et al., 1993). Finally, the actin-activated ATPase activity and the motor activity of the wild-type recombinant myosin are very similar to embryonic chicken myosin isolated from breast muscle or from primary culture myotubes, samples enriched for the chicken gene product.

There are very few expression systems available for site-directed mutagenesis experiments on muscle myosin. *Dicotylestium discoideum* has been used extensively and very successfully with nonmuscle myosin (Spudich, 1989, 1995), and recently, the baculovirus expression system has been applied to smooth muscle myosin and cardiac myosin (Sweeney et al., 1994; Trybus, 1994). However, neither of these systems has been very successful with a fast skeletal muscle myosin. The level of expression obtained with C2 cell line is comparable to these other systems. Furthermore, this unique system has the added advantage that the myosin incorporates into the endogenous cytoarchitecture, making it possible to analyze features specific to the assembly of the muscle-specific isoforms of myosin.

Rationale for Mutagenesis of Glycine 699

Our main goal was to analyze the role of a highly conserved glycine (G699) found in a turn that links the two reactive sulfhydryls by replacing it with an alanine to limit mobility about this highly conserved residue. The motor activity of the mutant myosin is dramatically affected by this point mutation, producing a >100-fold decrease in the sliding velocity of actin filaments. The rationale for selection of this specific site was based on the myosin structure (Fig. 10). Motion between the reactive sulfhydryls, SH1 and SH2, has been observed and analyzed (Wells et al., 1980; Dalbey et al., 1983). The separation of these sulfhydryl groups is influenced by nucleotide binding, and conversely, modification or cross-linking of these sulfhydryls can modify ATPase activity and actin binding affinity and can trap nucleotide (Reisler et al., 1974; Pemrick and Weber, 1976; Wells and Yount, 1979; Dalbey et al., 1983). In the myosin structure, these residues (C707 and C697) are located on well-defined α-helix segments that are joined by a turn that produces an 80° bend between the two helices and places the sulfhydryl groups 18 Å apart (Rayment et al., 1993b). In this turn, the conserved glycine (G699) is

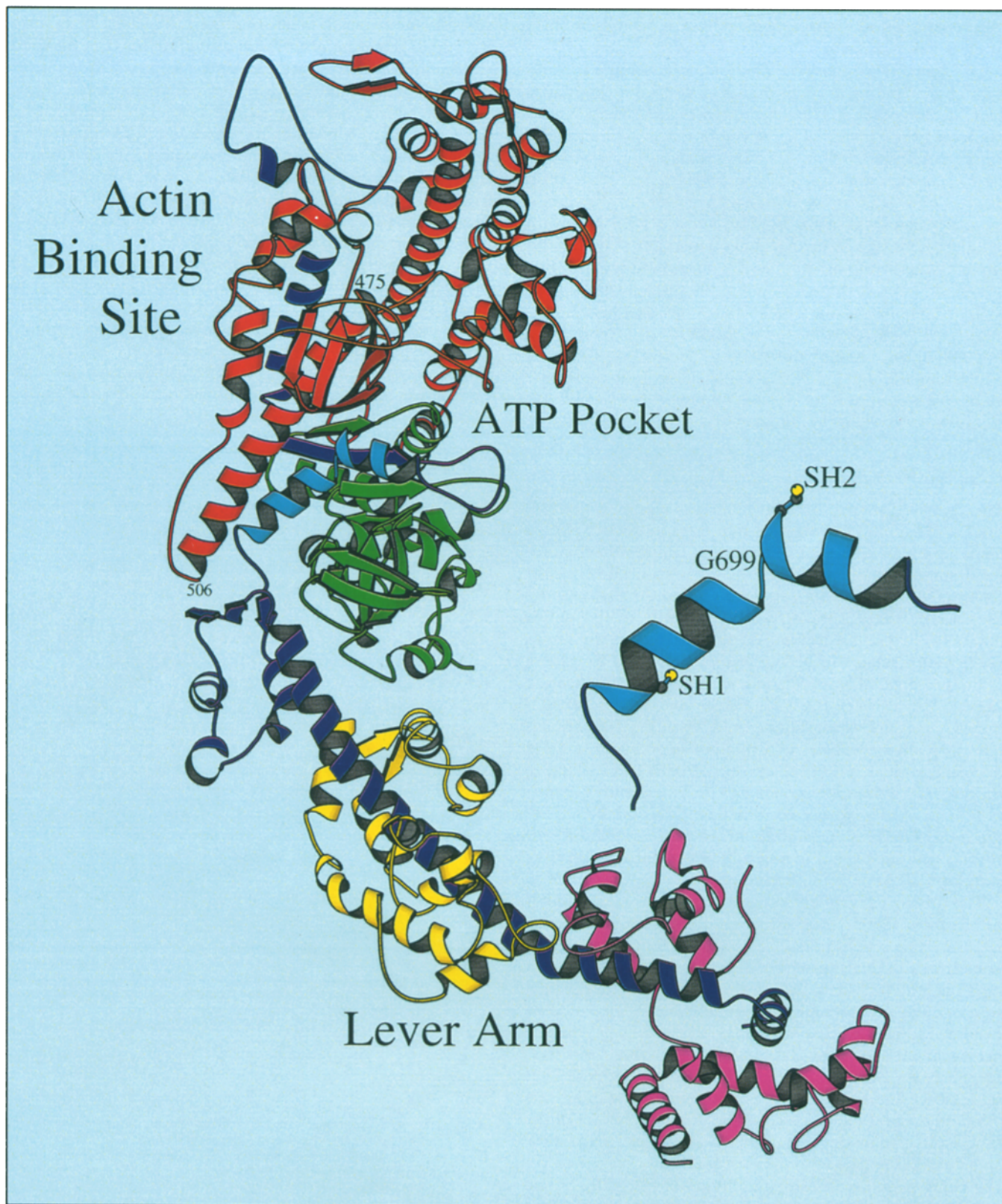


Figure 10. A ribbon representation of the structure of myosin S1. The model is oriented to highlight the two short helices that contain the reactive sulfhydryls, SH1 and SH2 (shown in light blue). The inset (residues 687–714) shows the position of the conserved glycine (G699) in the turn linking the reactive sulfhydryl helices. The highly conserved helix (475–506) that originates in the cleft and may provide a link to the SH1 helix is labeled. The motion of the lever arm is in-and-out of the plane of this diagram. This figure was prepared with the molecular graphics program MOLSCRIPT (Kraulis, 1991).

ideally situated to act as a pivot point for relative motion of these two helices.

The short SH1 helix (700–709) is directly linked to the light chain binding domain that acts as a semi-rigid lever arm. Motion of the SH1 helix could provide a direct link to the lever arm. This small helix also interacts with a longer, highly conserved helix (475–506) that originates in the cleft near the γ -phosphate site beneath the nucleotide pocket. This helix is contiguous with and underlying a major element of the actin binding surface (517–543) and could be sensitive to changes involving cleft opening and closure, nucleotide binding, and γ -phosphate release. Recently, domain movements that include the reactive sulfhydryl segment and the highly conserved cleft helix (475–506) have been reported in the structure of myosin head fragments with bound nucleotides (Fisher et al., 1995; Smith and Rayment, 1995). This suggests that these elements play an important role in coupling the actin and nucleotide binding sites to the lever arm.

Is G699 a Pivot Point?

The dramatic change in actin filament velocity caused by the G699A mutation suggests that motion about G699 is essential for coupling conformational changes in the motor domain with movement of the lever arm. The effect of the G699A mutation appears restricted to the motor activity without altering the structural integrity of the motor domain. The G699A mutant myosin folds normally, binds light chains, retains its ability to bind actin and to release in the presence of MgATP, and, although it is significantly slower, still powers the sliding movement of actin filaments. The G699A mutation could have this dramatic effect on filament velocity in a number of ways: (a) a large decrease in the length of the power stroke (from 10 nm to 0.1 nm); (b) a dramatic slowing of the rate-limiting transition in the ATPase cycle, resulting in a 100-fold increase in the total cycle time; (c) a dramatic increase in the duty ratio (i.e., the time spent in a tightly bound force generating state); or (d) some combination of these.

The mixing experiment shows that even a small number of the slow G699A mutant myosin crossbridges impede faster-cycling crossbridges. This suggests that the predominant effect is not a shortening of the power stroke, since, if only the length of the power stroke were affected, the mixture of adult myosin and mutant G699A myosin would be expected to move at the velocity of the faster myosin. The actin-activated ATPase data indicate that there is a five-fold increase in the total cycle time for the mutant. This increase is significant but is not sufficient to explain the 100-fold decrease in velocity or the dominant effect of the mutant in the mixing experiment. However, if the time spent tightly bound to actin is dramatically increased for the G699A mutant, then a small number of tightly bound crossbridges would have a dominant inhibitory effect on the fast-cycling crossbridges as is observed. Furthermore, a large change in the duty ratio would also give rise to persistent motion at the saturated velocity on low density myosin surfaces, a feature that also is observed with the G699A mutant myosin.

Dissociation of ADP at the end of the myosin ATPase cycle is necessary for rebinding of ATP to trigger the tran-

sition of a strong to weak binding interaction of myosin with actin. The rate of this step is limiting for the unloaded shortening velocity of muscle contraction or sliding movement of actin filaments in vitro (Siemankowski et al., 1985). We have concluded that this step is inhibited in the G699A mutant. A pivoting movement of the lever arm has been observed for an ADP-bound state of the acto-myosin complex (Jontes et al., 1995; Whittaker et al., 1995). Together, these data suggest a model where G699 acts as a pivot point for coupling movements in the motor domain to lever arm motion.

This region of the myosin structure is conserved in all members of the myosin gene family. Even in myosin gene families that lack the extended α -helical light chain binding domain that forms the lever arm, a carboxyl-terminal extension is always found that substitutes for this domain (Hammer, 1991; Wolenski, 1995), suggesting that this mechanism may be common to all myosin gene family members.

We are very grateful to Drs. M. Magnasco and L. Bourdieu for their efforts in developing the software, and Dr. D.J. Foran for help setting up and managing the motion-tracking software. We are also indebted to Dr. J.E. Schwarzbauer for plasmids, advice, and critical reading of this manuscript, and Dr. R.L. Trelstad for support, advice, and constructive suggestions.

This work was supported by Public Health Service grant AR38454 (to D.A. Winkelmann) and a grant from the American Heart Association—New Jersey Affiliate (to D.A. Winkelmann).

Received for publication 7 March 1996 and in revised form 17 May 1996.

References

- Bourdieu, L., M.O. Magnasco, D.A. Winkelmann, and A. Libchaber. 1995. Actin filaments on myosin beds: the velocity distribution. *Phys. Rev. E* 52: 6573–6579.
- Bouvagnet, P.F., E.E. Strehler, G.E. White, M.A. Strehler-Page, B. Nidal-Ginard, and V. Mahdavi. 1987. Multiple positive and negative 5' regulatory elements control the cell-type-specific expression of the embryonic skeletal muscle myosin heavy-chain gene. *Mol. Cell. Biol.* 7:4377–4389.
- Cheney, R.E., M.A. Riley, and M.S. Mooseker. 1993. Phylogenetic analysis of the myosin superfamily. *Cell Motil. Cytoskeleton* 24:215–223.
- Dalbey, R.E., J. Weiel, and R.G. Yount. 1983. Forster energy transfer measurements of thiol 1 and thiol 2 distances in myosin subfragment 1. *Biochemistry* 22:4696–4706.
- Domann, R., and J. Martinez. 1995. Alternative to cloning cylinders for isolation of adherent cell clones. *Biotechniques* 18:594–595.
- Finer, J.T., R.M. Simmons, and J.A. Spudich. 1994. Single myosin molecule mechanics: piconewton forces and nanometre steps. *Nature (Lond.)* 368:113–119.
- Fisher, A.J., C.A. Smith, J.B. Thoden, R. Smith, K. Sutoh, H.M. Holden, and I. Rayment. 1995. X-ray structures of the myosin motor domain of *Dictyostelium discoideum* complexed with MgADP.BeFx and MgADP.AIF⁻⁴. *Biochemistry* 34:8960–8972.
- Hammer, J.A., III. 1991. Novel myosins. *Trends Cell Biol.* 1:50–55.
- Itakura, S., H. Yamakawa, Y.Y. Toyoshima, A. Ishijima, T. Kojima, Y. Harada, T. Yanagida, T. Wakabayashi, and K. Sutoh. 1993. Force-generating domain of myosin motor. *Biochem. Biophys. Res. Commun.* 196:1504–1510.
- Jontes, J.D., E.M. Wilson-Kubalek, and R.A. Milligan. 1995. A 32° tail swing in brush border myosin 1 on ADP release. *Nature (Lond.)* 378:751–753.
- Kishino, A., and T. Yanagida. 1988. Force measurements by micromanipulation of a single actin filament by glass needles. *Nature (Lond.)* 334:74–76.
- Kodama, T., K. Fukui, and K. Kometani. 1986. The initial phosphate burst in ATP hydrolysis by myosin and subfragment-1 as studied by a modified malachite green method for determination of inorganic phosphate. *J. Biochem. (Tokyo)* 99:1465–1472.
- Kraulis, P.J. 1991. MOLSCRIPT: a program to produce both detailed and schematic plots of protein structures. *J. Appl. Cryst.* 24:946–950.
- Laemmli, U.K. 1970. Cleavage of structural proteins during the assembly of the head of bacteriophage T4. *Nature (Lond.)* 227:680–685.
- Lowe, S. 1994. The structure of vertebrate muscle myosin. In *Myology*. A.G. Engel and C. Franzini-Armstrong, editors. McGraw-Hill Book Co., New York. 485–505.
- Lowe, S., G.S. Waller, and K.M. Trybus. 1993a. Function of skeletal muscle myosin heavy and light chain isoforms by an in vitro motility assay. *J. Biol. Chem.* 266:20414–20418.

- Lowey, S., G.S. Waller, and K.M. Trybus. 1993b. Skeletal muscle myosin light chains are essential for physiological speeds of shortening. *Nature (Lond.)*. 365:454–456.
- Molina, M.I., K.E. Kropp, J. Gulick, and J. Robbins. 1987. The sequence of an embryonic myosin heavy chain gene and isolation of its corresponding cDNA. *J. Biol. Chem.* 262:6478–6488.
- Moncman, C.L. 1993. Molecular Analysis of Myosin Synthesis and Assembly. Rutgers University, New Brunswick, NJ. 200 pp.
- Moncman, C.L., H. Rindt, J. Robbins, and D.A. Winkelmann. 1993. Segregated assembly of muscle myosin expressed in nonmuscle cells. *Mol. Biol. Cell.* 4: 1051–1067.
- Pemrick, S., and A. Weber. 1976. Mechanism of inhibition of relaxation by *N*-ethylmaleimide treatment of myosin. *Biochemistry.* 15:5193–5198.
- Rayment, I., H.M. Holden, M. Whittaker, C.B. Yohn, M. Lorenz, K.C. Holmes, and R.A. Milligan. 1993a. Structure of the actin-myosin complex and its implications for muscle contraction. *Science (Wash. DC)*. 261:58–65.
- Rayment, I., W.R. Rypniewski, K. Schmidt-Base, R. Smith, D.R. Tomchick, M.M. Benning, D.A. Winkelmann, G. Wesenberg, and H.M. Holden. 1993b. The three-dimensional structure of a molecular motor, myosin subfragment-1. *Science (Wash. DC)*. 261:50–58.
- Reisler, E., M. Burke, S. Himmelfarb, and W.F. Harrington. 1974. Spatial proximity of the two essential sulfhydryl groups of myosin. *Biochemistry.* 13: 3837–3840.
- Robbins, J., T. Horan, J. Gulick, and K. Kropp. 1986. The chicken myosin heavy chain family. *J. Biol. Chem.* 261:6606–6612.
- Sambrook, J., E.F. Fritsch, and T. Maniatis. 1990. Molecular Cloning: A Laboratory Manual. Cold Spring Harbor Laboratory, Cold Spring Harbor, NY. 545 pp.
- Siemankowski, R.F., M.O. Wiseman, and H.D. White. 1985. ADP dissociation from actomyosin subfragment 1 is sufficiently slow to limit the unloaded shortening velocity in vertebrate muscle. *Proc. Natl. Acad. Sci. USA.* 82: 658–662.
- Silberstein, L., S.G. Webster, M. Travis, and H.M. Blau. 1986. Developmental progression of myosin gene expression in cultured muscle cells. *Cell.* 46: 1075–1081.
- Smith, C.A., and I. Rayment. 1995. X-ray structure of the magnesium(II)-pyrophosphate complex of the truncated head of *Dictyostelium discoideum* myosin to 2.7 Å resolution. *Biochemistry.* 34:8973–8981.
- Southern, P.J., and P. Berg. 1982. Transformation of mammalian cells to antibiotic resistance with a bacterial gene under control of the SV40 early region promoter. *J. Mol. Appl. Genet.* 1:327–341.
- Spudich, J.A. 1989. In pursuit of myosin function. *Cell Regul.* 1:1–11.
- Spudich, J.A. 1995. How molecular motors work. *Nature (Lond.)*. 372:515–518.
- Strehler, E.E., M.-A. Strehler-Page, J.-C. Perriard, M. Perisamy, and B. Nadal-Ginard. 1986. Complete nucleotide and encoded amino acid sequence of a mammalian myosin heavy chain gene: evidence against intron-dependent evolution of the rod. *J. Mol. Biol.* 190:291–317.
- Sweeney, L.H., A.J. Straceski, L.A. Leinwand, B.A. Tikunov, and L. Faust. 1994. Heterologous expression of a cardiomyopathic myosin that is defective in its actin interaction. *J. Biol. Chem.* 269:1603–1605.
- Trybus, K.M. 1994. Regulation of expressed truncated smooth muscle myosins. *J. Biol. Chem.* 269:20819–20822.
- Uyeda, T.Q., and J.A. Spudich. 1993. A functional recombinant myosin II lacking a regulatory light chain-binding site. *Science (Wash. DC)*. 262:1867–1870.
- Uyeda, T.Q. P., P.D. Abramson, and J.A. Spudich. 1996. The neck region of the myosin motor domain acts as a lever arm to generate movement. *Proc. Natl. Acad. Sci. USA.* 93:4459–4464.
- VanBuren, P., G.S. Waller, D.E. Harris, K.M. Trybus, D.M. Warshaw, and S. Lowey. 1994. The essential light chain is required for full force production in skeletal muscle myosin. *Proc. Natl. Acad. Sci. USA.* 91:12403–12407.
- Waller, G.S., G. Ouyang, J. Swafford, P. Vibert, and S. Lowey. 1995. A minimal motor domain from chicken skeletal muscle myosin. *J. Biol. Chem.* 270: 15348–15352.
- Warrick, H.M., and J.A. Spudich. 1987. Myosin structure and function in cell motility. *Annu. Rev. Cell Biol.* 3:379–421.
- Wells, J.A., and R.G. Yount. 1979. Active site trapping of nucleotides by crosslinking two sulfhydryls in myosin subfragment 1. *Proc. Natl. Acad. Sci. USA.* 76:4966–4970.
- Wells, J.A., M.C. Sheldon, M.M. Werber, and R.G. Yount. 1980. Crosslinking of myosin S1. *J. Biol. Chem.* 255:11135–11140.
- Whittaker, M., E.M. Wilson-Kubalek, J.E. Smith, L. Faust, R.A. Milligan, and L. Sweeney. 1995. A 35-Å movement of smooth muscle myosin on ADP release. *Nature (Lond.)*. 378:748–751.
- Winkelmann, D.A., and S. Lowey. 1986. Probing myosin head structure with monoclonal antibodies. *J. Mol. Biol.* 188:595–612.
- Winkelmann, D.A., S. Lowey, and J.L. Press. 1983. Monoclonal antibodies localize changes on myosin heavy chain isozymes during avian myogenesis. *Cell.* 34:295–306.
- Winkelmann, D.A., F. Kinose, and A.L. Chung. 1993. Inhibition of actin filament movement by monoclonal antibodies against the motor domain of myosin. *J. Muscle Res. Cell Motil.* 14:452–467.
- Winkelmann, D.A., L. Bourdieu, A. Ott, F. Kinose, and A. Libchaber. 1995. Flexibility of myosin attachment to surfaces influences F-actin motion. *Biophys. J.* 68:2444–2453.
- Wolenski, J.S. 1995. Regulation of calmodulin-binding myosins. *Trends Cell Biol.* 5:310–316.
- Yaffe, D., and O. Saxel. 1977. Serial passaging and differentiation of myogenic cells isolated from dystrophic mouse muscle. *Nature (Lond.)*. 270:725–727.